Ember risk modelling for improved wildfire risk management in the peri-urban fringes

Author

Roberts, Melanie E, Rawlinson, Andrew A, Wang, Ziyuan

1   Graphical Abstract
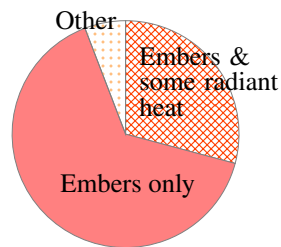
2   **Ember risk modelling for improved wildfire risk management in the peri-urban fringes**

3   Melanie E. Roberts,Andrew A. Rawlinson,Ziyuan Wang

Origin house loss & damage

Other

Embers & some radiant heat

Embers only

Radiant-heat & direct flame contact are typically the focus of asset protection measures.

However, embers are the leading cause of house loss and damage.

New model for ember risk: Convolving ember production with ember dispersal indicates hazard due to embers.

Symbols for diagrams courtesy of the Integration and Application Network (`ian.umces.edu/symbols`)   .

Highlights

Ember risk modelling for improved wildfire risk management in the peri-urban fringes

Melanie E. Roberts,Andrew A. Rawlinson,Ziyuan Wang

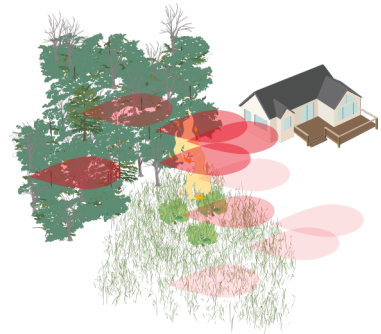- Developed new household level model for risk posed by embers
- Scalable model with minimal data requirements
- Application of the model demonstrated for the 2015 Warringine Park bushfire, Victoria, Australia

Ember risk modelling for improved wildfire risk management in the peri-urban fringes

Melanie E. Roberts[a,b,*,1], Andrew A. Rawlinson[c] and Ziyuan Wang[d,1]

[a]*Australian Rivers Institute, Griffith University, 4111, Australia*

[b]*School of Mathematics and Statistics, University of Melbourne, 3010, Australia*

[c]*IBM Research - Australia, 60 City Road, Southbank, 3006, Australia*

[d]*Digital Research Innovation Capability Platform, Swinburne University of Technology, 3122, Australia*

ABSTRACT

Although embers are a leading cause of house loss and damage from wildfire, risk reduction activities such as vegetation management and planning requirements do not adequately account for the risk of embers. To help address this, a model of the potential ember risk is presented. It takes into account local vegetation and background wind conditions for both long-range and short-range ember dispersal. This model is developed to provide indications of the importance of embers to the household-level wildfire risk in communities at the wildland-urban interface. The model provides information for householders to improve understanding of the nature of ember risk within the community, and to assist planning in order to respond to that risk. A case study of the 2015 Warringine Park (Coastal Section) bushfire in Australia is presented, which demonstrates how the model could be used to assist with community planning. The utility of this outcome for community and household level wildfire planning and preparation is discussed.

1. Introduction

The destruction and damage of properties due to wildfire is a growing problem in many regions (Syphard et al., 2012; Chuvieco et al., 2013). Damages in numerous fire events globally have been attributed to ember activity over radiant heat and direct flame losses (Blanchi and Leonard, 2005; Handmer and Tibbits, 2005; Maranghides and Mell, 2010; Cohen, 2012; Westhaver, 2017).

Given the leading role of embers in house loss and damage due to wildfire, it is essential that practices to mitigate risk directly address the component of risk due to embers. It is somewhat surprising that embers do not hold a central role in some mitigation activities. In Australia, houses more than 100 meters from bushfire prone vegetation require no special construction standards (Standards Australia, 2009, AS3959). This focus on radiant heat and direct flame contact can also be seen in the management of vegetation by local government authorities. Following the 2015 Warringine Park bushfire near Melbourne, Australia, where 32 properties were damaged from ember activity, a review found the Fuel Management Zones were found to have performed satisfactorily, as they 'achieved the objective of preventing radiant heat and flame ignition of houses from a fire in the reserve' (Terramatrix, 2015, p. 3) with losses due to embers appearing not to be a key concern.

This focus away from ember risks is not universal. For example, the State of California introduced ignition-resistant standards to their building code that will protect buildings from being ignited by flying embers (Cal Fire, n.d.a). Public education campaigns are used to inform residents about the risks posed by embers, and to encourage homeowners to take action to reduce their risk. This information, often delivered via brochures or online material from local firefighting agencies, provides generic advice to homeowners (see for example Country Fire Authority (2011); Cal Fire (n.d.b)). Internet-based solutions provide opportunities to deliver more personalised advice to homeowners with minimal overhead, adapting to local factors and the preferences of the individual user. One example is the app PREP: Personalised Recommendations for Emergency Management, described by Wang et al. (2016). This app is designed to provide residents with both their long term and immediate wildfire risk, while providing individualised recommendations for how to mitigate that risk. Through the app, residents can explore the expected risk reduction they could achieve through different combinations of mitigation strategies. Taking a longer-term approach, recommendations such as installing window shutters or upgrading their fences to metal are given, with indications of the expected benefit and cost of such actions. In the short term, residents are alerted to high risk conditions and assisted in stepping through their fire plan, where the expected benefit and effort of different actions is highlighted, to assist in the prioritisation of tasks. Visualising changing risk can assist individuals and communities to better respond to wildfire. Importantly, PREP was developed to absorb the computational burden of calculating risk from homeowners. This means that users should not have to take measurements, or access data not typically available to them in order to use the app.

To be effective, apps such as PREP require a comprehensive model of risk that captures the key contributions to that risk. The role of embers in house loss and damage makes it imperative that embers are explicitly included in the underlying risk and mitigation models. To be effectively included in an app like PREP, the model for ember risk must satisfy the following criteria:

- available in the public domain for use by third-parties;

- require only data publicly available or commonly known to residents;

- be computationally light, able to be rapidly updated across large spatial extents simultaneously; and

- provide actionable information about the ember component of wildfire risk to properties.

A suitable model of the contributions of embers to risk does not exist. Although a number of models of household risk have been developed, they do not meet one or more of the above criteria. Existing models include the Structure Ignition Assessment Model (SIAM) (Cohen, 1995), the Bushfire Attack Level (NSW Rural Fire Service, 2012), Wilson's (1988) House Survival Likelihood Function and Tolhurst and Howlett's (2003) House Ignition Likelihood Index.

We therefore developed a new model of ember risk to better inform household and community planning around wildfire risk. Our model takes information about ember-producing vegetation in the area, together with how those

embers will disperse under different wind conditions, to determine the potential for embers to impact a property, were a wildfire to occur. This model is designed to be one component in an overall model of wildfire risk of a property. The ember risk model will complement models capturing other aspects of wildfire risk, such as temperature and humidity, radiant heat, and direct flame contact. The objectives of the developed model are to:

- capture the dominant factors of ember risk;

- provide actionable information to homeowners;

- require only publicly available data;

- be able to leverage advances in scientific knowledge of embers and high-fidelity data where available, but not be reliant on this information; and

- be suitable for incorporation in an app like PREP (see requirements above).

Our developed model differs from previous approaches to ember risk in that it focuses on the potential load of embers impacting a property, and employs a mathematical framework that is adaptable to the quality of information available in different geographic regions. The model provides an important first step to community-wide indications of ember risk, to assist personalised and group risk mitigation activities.

This paper is organised as follows. In the remainder of this section we provide an overview of related work and key considerations of ember risk. In Sec. 2 we introduce the mathematical model to describe the potential ember load impacting a property, which relates distribution of ember production to the dispersal of embers via convolution. We consider two possible dispersal functions. Sec. 2.1 examines short-range dispersal, with an application of the model to the 2015 Warringine Park bushfire. Sec. 2.2 considers long-range ember transport, which is illustrated via application to a simulated housing estate. This is followed by an overview of the software framework in Sec. 3 before comment on the applicability of the model in Sec. 4. We conclude with a summary and discussion of future work in Sec. 5.

1.1. Related Work

In addition to the impacts of embers on properties, embers are responsible for accelerating the fire front and creating spot fires (MacAuley, 2003), which generate significant challenges for fire suppression. The role of embers in fire progression has motivated a considerable body of research, including ember generation and ember size (e.g. Ellis (2000); Manzello et al. (2009); Suzuki et al. (2012); Manzello and Foote (2012); Hall et al. (2015)), flight and spotting distance (e.g. Albini (1983); Woycheese et al. (1999); Anthenien et al. (2006); Koo et al. (2012); Harris (2011); Wang (2011); Thurston et al. (2017)), ignition on landing (Tarifa et al. (1965); Manzello et al. (2006)), and how to incorporate embers in fire modelling products (e.g. Rothermel (1983); MacAuley (2003); Alexandridis et al. (2008); Chong et al.

(2012); Perryman et al. (2013); Dold et al. (2014)). This research has predominantly focussed on spot fires and the coalescence of the fire front, however attention has also been paid to the risk of structures igniting due to embers.

1.2. Ember risk model considerations

The ember risk of a property refers to the likelihood that a property will sustain damage as a result of embers. The ember risk of a property is a function of many factors of the built and natural environment, and is further influenced by the decisions made by agencies and residents of the surrounding community. Factors of the built environment include choice of building materials, the shape and orientation of homes, distance between structures, and the presence of shade sails, decks and pergolas. Other factors directly controlled by property owners and occupants include the availability of firefighting resources such as water supplies, hoses, pumps and generators, and access to the property for firefighting. The influence of the built environment on wildfire losses has been extensively studied (Manzello and Suzuki, 2013; Syphard et al., 2012; Handmer and Tibbits, 2005; Gibbons et al., 2012; Papakosta et al., 2017).

Factors of the natural environment that affect the ember risk include the location and characteristics of vegetation in the region, topography and weather. Key vegetation characteristics include the fine fuel load and the nature of embers that will be produced in terms of their typical spotting distances and densities.

The household garden is also a critical factor in the ember risk of a property. The proximity of plants to houses or other structures and the propensity of vegetation to either screen or fuel fires from embers is critical (see for example Cal Fire (n.d.b); Country Fire Authority (2011); Quarles and Smith (2011)). Defensive actions, taken by residents and firefighters, will further impact whether the ember risk is realised. The active defence of a property, particularly from ember attack, has been identified as a critical factor in the likelihood of properties surviving a wildfire (Wilson and Ferguson, 1984; Beringer, 2000).

The contribution of these factors to the total ember risk of a property is complex, and requires a large volume of information, much of which is not generally available or able to be derived from public data sources. We therefore restrict our model to those features that can be derived from public data sources, and incorporate factors of the built environment and home as adjustments to the risk applied by the resident as in Wang et al. (2016). This work therefore focuses on factors of the natural environment that contribute to the potential ember load a property may be subjected to during a wildfire, specifically wind speed and direction and the distribution of vegetation.

The ember hazard of a property is therefore defined as the potential ember load that it could be subject to during a wildfire, because of local forest such as national parks, state parks, and community green spaces, while acknowledging that this does not tell the complete story for risk. A wildfire will not necessarily ignite all areas of a forest surrounding a community. Embers will only be produced where the fire is locally sufficient to ignite the fuels. Importantly, not every ember remains alight (Ganteaume et al., 2011), or lands on flammable material, and hence the majority of embers

may not be viable to spread a wildfire to a property. The ember load may therefore be considered an approximate upper bound; if the hazard from the ember load is high it is important to ensure the property is resilient to ember attack, whereas if the hazard is very low such features are less critical. The calculated ember load provides a density of embers, or scaled number per unit area, however we stress that the ember load should not be taken as a prediction of the specific count of embers, but rather whether many (high hazard) or very few (low hazard) embers could be expected. The measurement is relative, and identifies areas of comparatively higher or lower risk within a region, or between regions. The ember load is therefore a model for the potential hazard posed by embers. It is assumed that an increase in the load of embers impacting a property will result in an increased likelihood that the property will be damaged, that is an increase in ember risk. The ember load is not a prediction of the damage a property will sustain, due to the many other factors that affect damage including the property's vulnerability and the effectiveness of defensive actions. A property is considered to be the area of private land surrounding a house, which includes the household garden (and pool, deck etc.). In urban areas, this is typically the area within the fence, while in more rural areas this is the managed area of land immediately around the home (sometimes referred to as the house yard).

To calculate the ember hazard of a property we consider two factors – the propensity of the forest in the area to produce embers, and the distribution of those embers under the prevailing wind conditions. Different types of vegetation produce different types and quantities of embers, while the shape, initial size, burning characteristics, and whether the ember is entrained in the plume or not, all affect the flight path of the ember (Anthenien et al., 2006). The bark, twigs, leaves, etc. that become embers all have different aerodynamic and flammability characteristics. For example, ribbon gums (*Eucalyptus viminalis*) are known for their bark, which hangs from trees in long streamers that are easily ignited and carried long distances from the point of ignition (Hall et al., 2015), whereas stringybark eucalyptus tend to produce more wood-chip like bark embers that are less likely to be lofted by the fire-plume and instead are typically associated with massive short-range spotting (MacAuley, 2003). These differences mean that different types of vegetation are more prone to producing embers that will pose a risk to properties due to how long they remain alight, how they fly, and the quantity of embers of each type produced. Rarely, however, is such detailed information about the vegetation in a wildfire prone region likely to be up to date and available, nor is there detailed knowledge of the flight paths and dispersal patterns of each type of ember. We therefore adopt some simplifications in the modelling to account for data limitations, while providing a framework that can take advantage of this information should it be available. These simplifications are introduced in the following paragraphs.

2. Ember load model

The method of convolution is used to identify the cumulative impact of a distribution of ember releases, transported according to a known dispersal function, on a property. We model the distribution of embers originating from a unit

area of forest by the probability density function (PDF) ρ_E, where the form of ρ_E is dependent on the underlying mechanisms spreading the embers. The ember distribution due to a forest η_{EF} is then obtained by convolving the number density function (NDF) of the forest η_F with the PDF for the embers ρ_E

$$
\begin{aligned}
\eta_{EF} &= (\rho_E * \eta_F)(x, y) \\
&= \int dx_1 \int dy_1 \rho_E(x_1, y_1) \eta_F(x - x_1, y - y_1),
\end{aligned}
\tag{1}
$$

where the NDF of the forest η_F describes the spatial distribution of the fine fuel load. Ideally, the NDF of the forest reflects the propensity of the vegetation to generate embers. Different classes of vegetation are known to differentially produce embers; the primary concern for ember production is typically the bark fuel load in forested areas. Spatial information about the ember production capabilities of a region is not typically available in public datasets. The ember production capabilities of a region are therefore approximated by the fine fuel load for this analysis. Where more detailed information is available, this should be used in preference to the fine fuel load.

Convolution enables us to sum across all vegetation in the area (represented by the integration of x_1 and y_1 in Eq. 1) to return the cumulative impact on the property of interest. Therefore, solution of Eq. (1) for a specific PDF to describe how embers are dispersed by the background winds and NDF describing the distribution of fine fuels within a region, gives the ember hazard for the property located at (x, y). To implement this model, the spatial distribution of the fine fuel load and of the target properties are required, together with the wind conditions (direction and speed) of interest. The fine fuel load should be discretised. The discretised fine fuel load (η_F) is then convolved with the PDF (ρ_E) under the defined wind conditions, producing as an output the spatial distribution of the potential ember load (η_{EF}). A pseudo-algorithm to describe this approach is provided in Appendix A. The ember load represents the hazard to a property from ember attack. This spatial distribution of ember load can be used to explore the ember hazard within a community, or at an individual property, under different conditions.

The ember load profile of a property provides an indication of how resilient to embers it needs to be.

The calculated ember load is a density and provides a relative map of the ember hazard in an area. While the ember load is representative of a number or count of embers, it does not provide the expected number of embers that will impact a property.

Information on the spatial distribution of embers originating from an area of burning vegetation is limited. Detailed observations of ember dispersal, relative to their origin, from wildfires is not available, and experimental results are limited. It is therefore necessary to assume the form of the PDFs based on the available information about ember dispersal. We consider two specific PDFs for ember distribution due to different mechanisms later in this section.

As indicated above, the fine fuel load is used to approximate the number of embers produced from an area of

vegetation during a fire. This is a simplification; the type of vegetation is as important as the fuel load in determining the appropriate density function. Two areas with the same fuel load may produce dramatically different numbers of embers. Consider for example a eucalypt forest with a high bark load versus grassland of the same fine fuel load. In this case, it would be expected that the eucalypt forest would produce more embers than the grassland. Moreover, the distribution of different types of embers (e.g. from candlebark versus stringybark trees, or grasses) under the same weather conditions will not be the same. The developed model and framework is flexible and can account for these differences, where sufficient information is known to form the distribution functions. If a forested region contains different types of vegetation, e.g. eucalypts and pine trees, each having their own embers PDFs and NDFs, the ember distribution due to such a heterogeneous forest is

$$
\eta_{EF}(x, y) = \left(\rho_E^{\text{Eucalyptus}} * \eta_F^{\text{Eucalyptus}} + \rho_E^{\text{Pines}} * \eta_F^{\text{Pines}} \right)(x, y). \tag{2}
$$

As a first approximation, we neglect the variation in the PDF due to different vegetation types, and therefore incorporate variation in the vegetation solely through the fuel load. Incorporating variation in the ember distribution due to vegetation types would require detailed information about how embers from different plant species are dispersed as a function of wind speed. This research exists for only a limited number of plant species and conditions (see for example Baker (2005); Manzello et al. (2007, 2008, 2009); El Houssami et al. (2016)). For practical implementation, the distribution of species throughout a region would also be required to take advantage of a more detailed distribution model. This information is not typically available through public datasets.

Two underlying mechanisms for ember spread are considered, referred to as short-range and long-range embers. While short-range embers can be lofted by thermals from the fire directly (Anthenien et al., 2006) and dispersed by background winds, long-range embers have the additional feature of being entrained in the buoyant fire plume before being dispersed. Fibrous bark, such as from eucalypt stringybark species (e.g. *E. obliqua*, *E. marginata* and *E. macrorhyncha*) is commonly associated with short-range spotting, while long-range spotting is typically due to long streamers of bark that normally hang from the upper regions of smooth-barked eucalypt species (e.g. *E. viminalis*, *E. globulus*, and *E. delegatensis*). These long bark pieces can stay alight for as long as 40 minutes (Cruz et al., 2012).

2.1. Short-range embers

Analysis of ember spots (burn marks) following wildfires indicates that the ember density decreases exponentially with distance from the vegetation (Ellis, 2003; Tolhurst and Howlett, 2003). These observations are consistent with the down-scaled experimental results presented by Zhou et al. (2015). Their results, which were reported as a function of the horizontal distance only, show a skewed Gaussian distribution with higher wind speeds corresponding to a flatter distribution with embers travelling further from the origin. Given the scale of the experiments, on the order of meters,

226 this result is not dissimilar to the exponential decay observed in the field.

227   We therefore assume that the probability density function for embers, due to short-range processes, is described by

$$\rho_{E_{\text{short}}} = \frac{\lambda^2}{\pi} \sqrt{\frac{\kappa}{u}} \, \exp\left(-\lambda \sqrt{\frac{\kappa}{u} x^2 + y^2}\right),$$ (3)

228 where u is the wind speed [m/s], and x and y are the distance [m] in the wind direction and transverse wind direction

229 respectively. The wind speed is nominally taken as the 10m wind speed, acknowledging that observations may be

230 recorded at a different height. In this paper we assume a spatially constant windspeed. This is a simplification of the

231 true situation. Not only does the wind speed vary spatially and with height above the ground, interactions with the

232 canopy and topography will vary the local windspeed (Allen, 2006; Belcher et al., 2012; Quill et al., 2019). This PDF

233 describes a distribution of embers that decreases exponentially with distance from the origin. The decay is skewed such

234 that embers travel preferentially in the wind direction. If $\kappa/u = 1$, this would describe a radially symmetric distribution.

235 κ [1/m] and λ [m/s] are scaling parameters, which are ideally determined from observations or more detailed modelling

236 of ember dispersal, but here have been assumed. The above equation assumes that the wind is travelling in the positive

237 x-direction, and thus a simple rotation is employed to account for variations in the wind direction. Fig. 1 shows the

238 assumed distribution of embers originating from a unit area of vegetation for three background wind speeds. Higher

239 wind speeds result in the embers being transported further from the fire, with the transverse spread decreasing. The

240 density function Eq. (3) was chosen as it represents embers that travel predominantly in the wind direction, with a

241 degree of spread in the transverse direction. The scaling parameter κ controls the transverse spread, with the parameter

242 λ giving the length scale over which the ember count decays. The density of embers decreases exponentially from the

243 origin, $(x, y) = (0, 0)$. As Eq. (3) is a probability density function, that is,

$$\int_0^\infty dx \int_{-\infty}^\infty dy \rho_{E_{\text{short}}} = 1$$ (4)

244 evaluating Eq. (3) over an area will return the fractional proportion of embers that fall within the area, relative to the

245 total number of embers produced.

246   Convolving the short-range ember PDF, Eq. (3), with a distribution of forest (fine-fuel load) as per Eq. (1) allows

247 us to explore the potential risk to a community in close proximity to bushland. This measure is dynamic, able to be

248 updated at the same frequency as the input data, and can be evaluated at the resolution of a single property. This

249 provides a fine-scaled measure of the potential ember load, able to reflect a variety of design scenarios. Design events

250 are useful to inform planning activities, where an event with a series of desired characteristics, or event likelihood

251 (such as the one in 100-year event), is modelled to identify the expected impact. This approach can be applied to the

252 ember load, however perhaps a more useful exercise from a homeowner's perspective is to understand where their risk
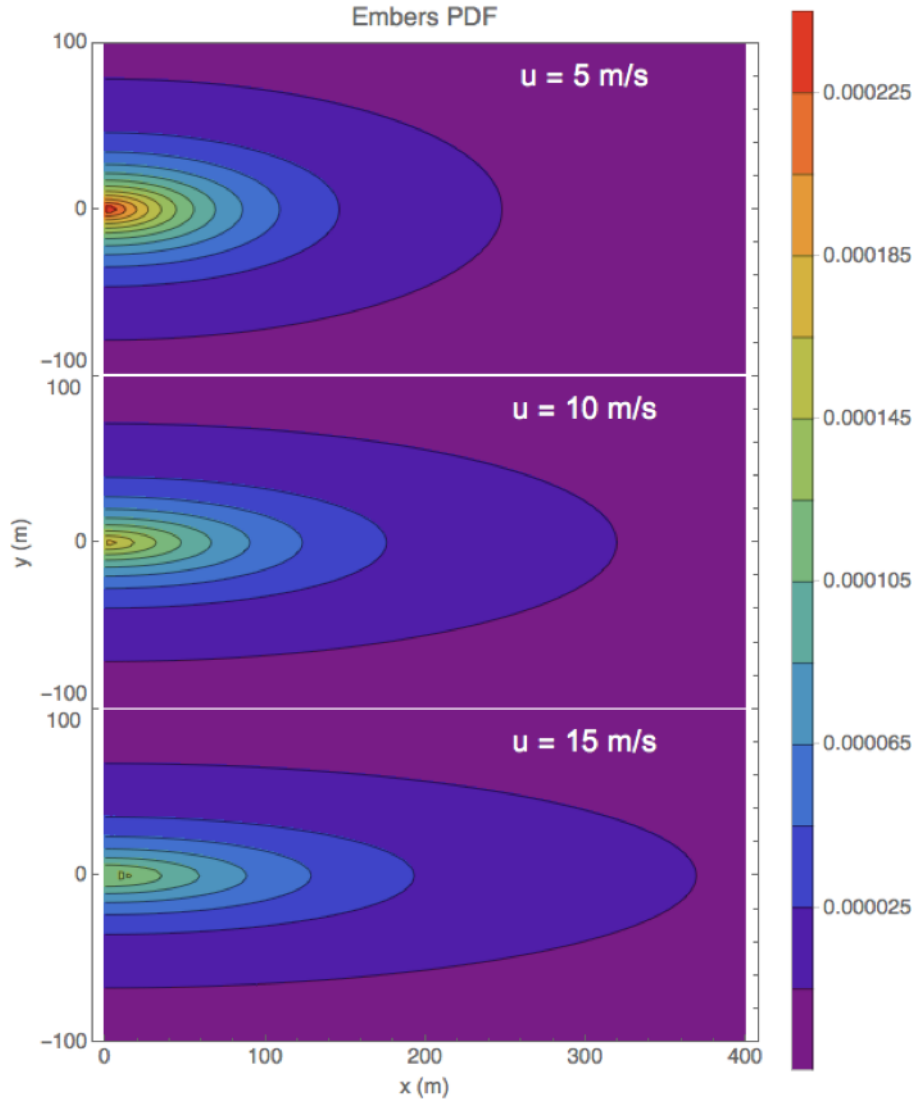
Figure 1: Assumed distribution of embers from a unit area of forest due to short-range mechanisms subject to three different background wind speeds u [m/s] in the positive x-direction, and with $\lambda = 0.5$ m/s, and $\kappa = 0.05$ 1/m. The warmer colours correspond to high concentrations of embers while the cooler colours correspond to lower concentrations of embers. The ember load is a density with units of scaled count per unit area. Embers are released from the origin (0,0), and the x- and y-axes are measured in m.

is coming from.

The shape and orientation of a home, placement of decks, driveways and water tanks, and the use or otherwise of screens, all affect the total wildfire risk of a property. Knowledge of the wind-direction that drives the dominant ember load impacting a property assists homeowners in trading the costs of risk reduction (financial, aesthetic and lifestyle) with the risk reduction achieved, while local councils and fire agencies can incorporate this information with their risk assessments to better manage public vegetation. The ember load for an example vegetation distribution under different

wind conditions is explored in Figs. 2 and 3. The potential ember load is calculated considering only short-range processes, that is with the ember density function given by Eq. (3), with a wind speed of 15.8 m/s. The parameter values $\lambda = 0.5$ m/s, and $\kappa = 0.05$ 1/m are used in these figures. These parameter values were selected to enable the model to be illustrated. Further data is required to parameterise the model with confidence. A Monte-Carlo approach is used to explore the sensitivity of the model to the selected parameter values.

Fig. 2 shows how different wind directions change the ember load at different locations within a community. Fig. 2 also shows how different areas of a community are differently impacted under constant wind conditions. The assumed vegetation distribution, consisting of a relatively high fuel load in the centre of the region surrounded by low fuel loads, results in a very high ember load under all wind directions for some locations. For other locations, the wind direction plays a key role, with the ember load varying from low to very high. Consider for example a property located at the reference location (1250,1500), where the load varies between very high (dark red) to low (dark blue), depending on the wind direction. In combination with local fire knowledge, a community level mapping of ember load can assist local council and fire response agencies with their risk mitigation activities. For example, councils can investigate the community wide impact of different vegetation management schemes, or consider the likelihood of ember attack in the positioning of community fire refuges, evacuation centres or neighbourhood safer places (see Country Fire Authority (2012)).

At the individual property level, Fig. 3 shows a radial plot of the ember load for a background wind speed of 15.8 m/s across sixteen wind directions for two sample property locations. This information will assist property owners in understanding their localised risk, and the conditions under which this risk is significant. Studies into wildfire preparedness have shown that people who are more knowledgeable about their fire risk, and hence have a higher perception of risk, are more likely to engage in mitigation activities (Beringer, 2000; Brenkert-Smith et al., 2012; McCaffrey, 2015), however perceiving the risk is a necessary but not sufficient condition for people taking protective actions (McCaffrey, 2015). By providing detailed information at the individual property level, homeowners can make informed decisions to mitigate their risk, given financial constraints, and without unduly compromising their lifestyle.

For the property in Fig. 3a, the risk is concentrated in the west to south-west sector, and thus an owner may choose to first screen windows and reduce vegetation on that side of the house to mitigate their risk. The property in Fig. 3b is at a much higher risk, with a non-negligible load in most wind directions. The western side of the house is most at risk, and therefore is a poor location for any structures such as water tanks, decks or sheds. In this case, the residents may choose to install a high metal fence to the west of the property, in addition to gutter and window screens, and locate their deck on the east side of the property. Such actions, informed by detailed property level risk measures, are likely to be more effective than applying generic measures for risk reduction. As discussed earlier, the ember load is just one component of wildfire risk, and therefore such information should be presented to homeowners together with
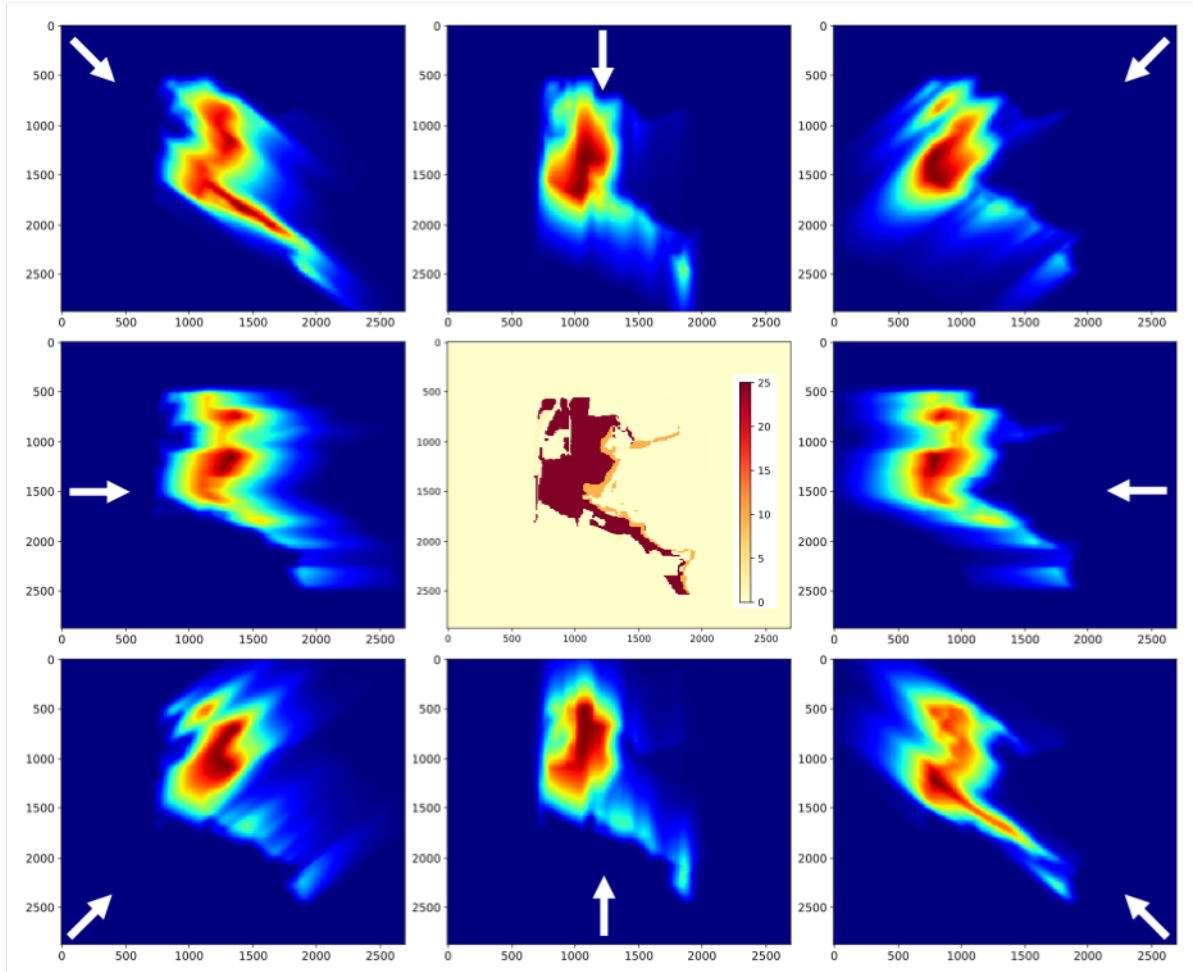
Figure 2: Ember load (units of scaled count per unit area) subject to a background wind speed of 15.8m/s in the eight cardinal and intercardinal directions. The centre figure shows the distribution of vegetation, with a non-uniform fuel load (fuel load in t/ha shown by the colour bar), with the eight external plots corresponding to the background wind direction (indicated by the white arrow), thus the top left figure is a north-westerly wind etc. Warm colours represent a high ember load with cooler colours representing a low ember load. The x and y axes show the relative positions within the area of interest in metres, an area of approximately 2.5km x 2.5km. The potential ember load is calculated considering short-range processes only. That is, with the ember PDF given by Eq. (3). The above figures are generated with $\lambda = 0.5\,\text{m/s}$, and $\kappa = 0.05\,1/\text{m}$.

other risk factors, for example as proposed in Wang et al. (2016).

Fig. 3 also provides an uncertainty analysis for the shape parameters λ and κ. A Monte Carlo approach with 100 replicates is shown. The parameters were randomly sampled from a log-normal distribution with means 0.05 and 0.1, and standard deviations 0.2 for λ and κ respectively. These results show that while the magnitude of the ember load varies with different parameter values the conclusions remain consistent. That is, the direction of principal risk for the properties is unchanged.
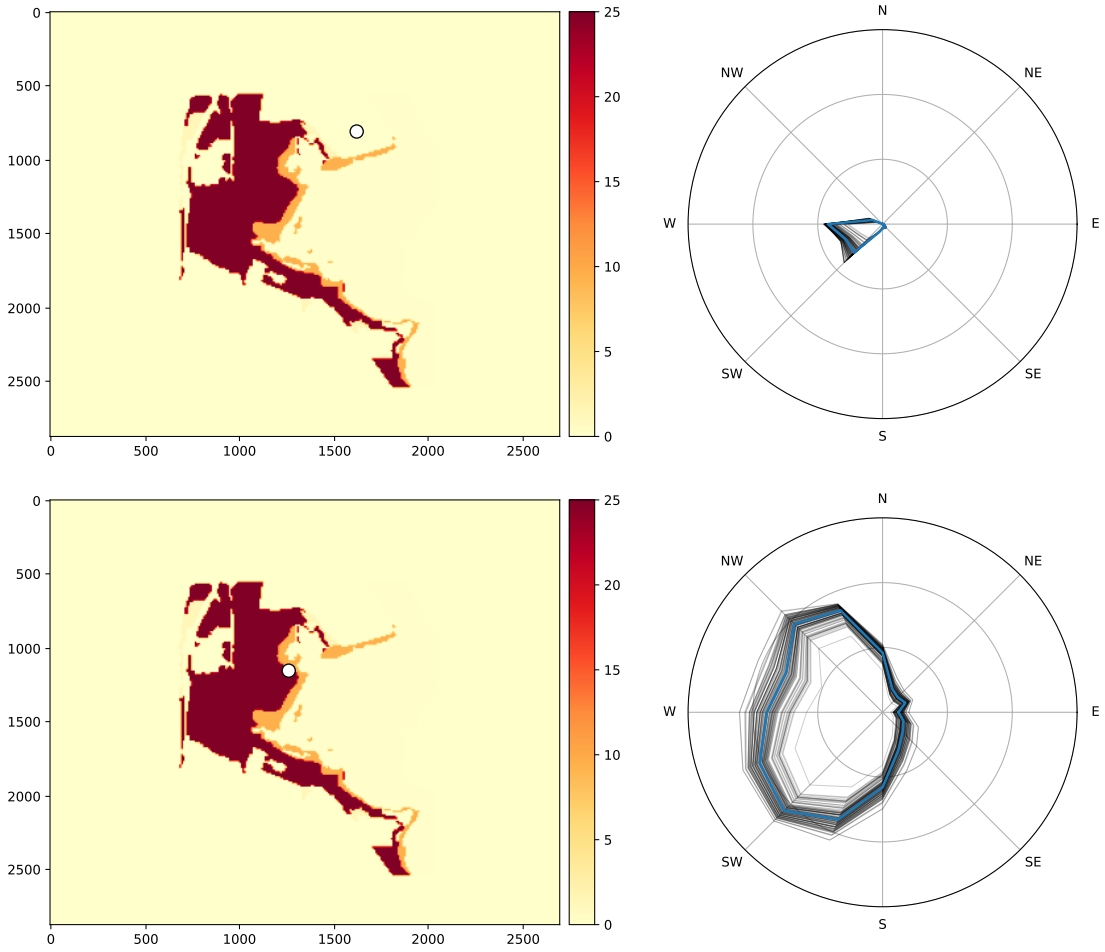
Figure 3: Directional ember load (units of scaled count per unit area) for two selected properties, indicated by the white dots, with a background wind speed of 15.8m/s, and a variable fuel load (t/ha). The circular plot indicates the wind direction corresponding to the risk, with the same scale used across both plots. The darker colours correspond to a higher fuel load, with lighter colours corresponding to a lower fuel load, the fuel load is indicated by the heat bar, with the darker brown corresponding to a fuel load of 25t/ha, the orange to a fuel load of 9.5t/ha, and the lighter yellow to fuel loads of less than 2t/ha. The x and y axes show the relative positions in metres within the area of interest, an area of approximately 2.5km x 2.5km. The potential ember load is calculated considering short-range processes only. That is, with the ember PDF given by Eq. (3). A Monte Carlo simulation with 100 runs is used to explore sensitivity to the parameters λ and κ, with each grey line corresponding to a single run. The blue line indicates the result with $\lambda = 0.5 \, \text{m/s}$, and $\kappa = 0.05 \, 1/\text{m}$.

2.1.1. Case study: Warringine Park bushfire

On the 3rd of January 2015 a fire to the north of Warringine Park (Coastal Section), in Victoria Australia, spread into the reserve under northerly winds. A westerly wind change late in the afternoon drove the eastern flank of the fire towards residential buildings in the suburb of Hastings, resulting in 32 properties being damaged (no properties were destroyed) and approximately 50% of the reserve being burnt. All property damage was found to have been due to ember activity, with no losses due to radiant heat or direct flame contact (Terramatrix, 2015). Following the bushfire, the Mornington Peninsula Shire Council commissioned a report focussing on four areas: fire behaviour,
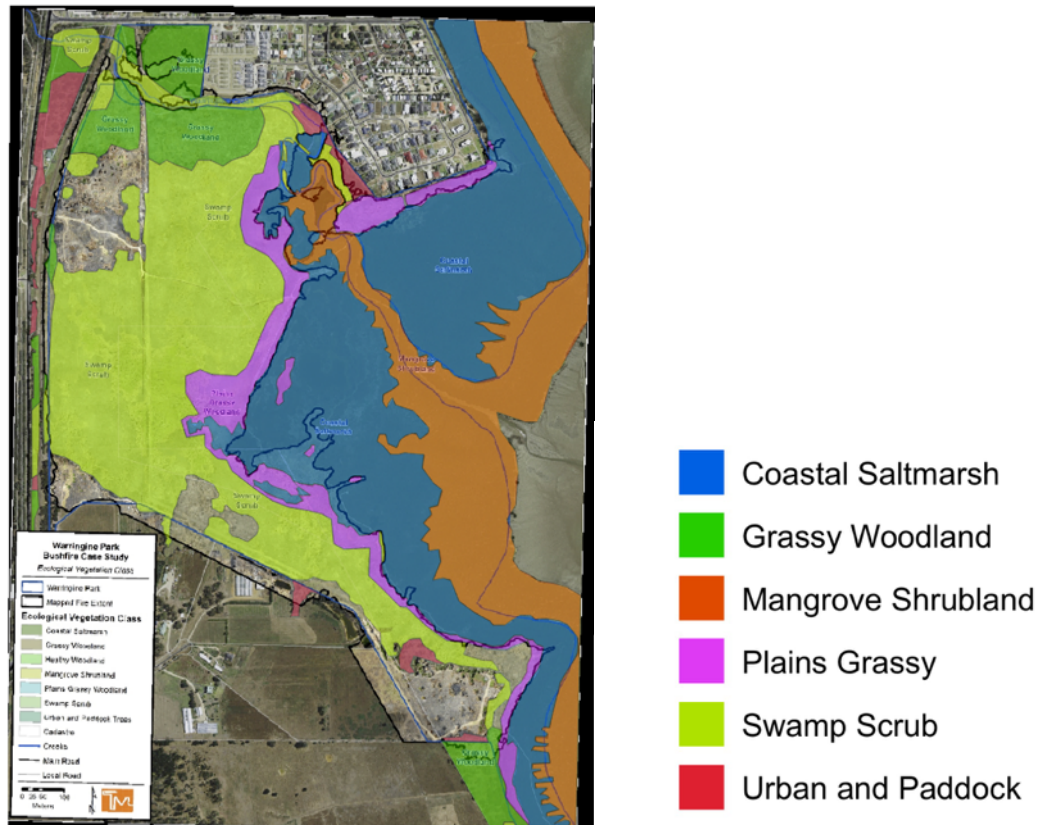
Figure 4: Assumed ecological vegetation classes for the Warringine Park bushfire case study. These are adapted from Terramatrix (2015b), shown overlaying the report's Map 2.

fuel management zones, community engagements and fire education, and land use planning and building controls (Terramatrix, 2015b). The vegetation (Map 2), fire progression (Map 6), and property damage (Map 9) maps, together with the fire behaviour and weather details provided by this report (Terramatrix, 2015b) form the basis of our case study.

These maps were manually digitised using the program Quantum GIS (QGIS, 2015). A uniform grid, with spacing 0.001 (equivalent to approximately 9m in the longitudinal and 11m in the latitudinal directions), was applied; the characteristics of the grid are assumed to be uniform and represented by the central point. Our digitised versions of the vegetation and fire progression maps are given in Figs. 4 and 5. Fig. 4 shows the assumed distribution of vegetation for each of the six identified vegetation classes. Heathy woodland, whilst identified in the key to Terramatrix (2015b, Map 2), was not able to be identified on the map, which may be due to the colour selection overlaying satellite imagery for the area obscuring the difference between different vegetation classes, or due to heathy woodland being absent from the mapped region.

The ember load experienced by properties due to the bushfire would have varied over time in response to changes
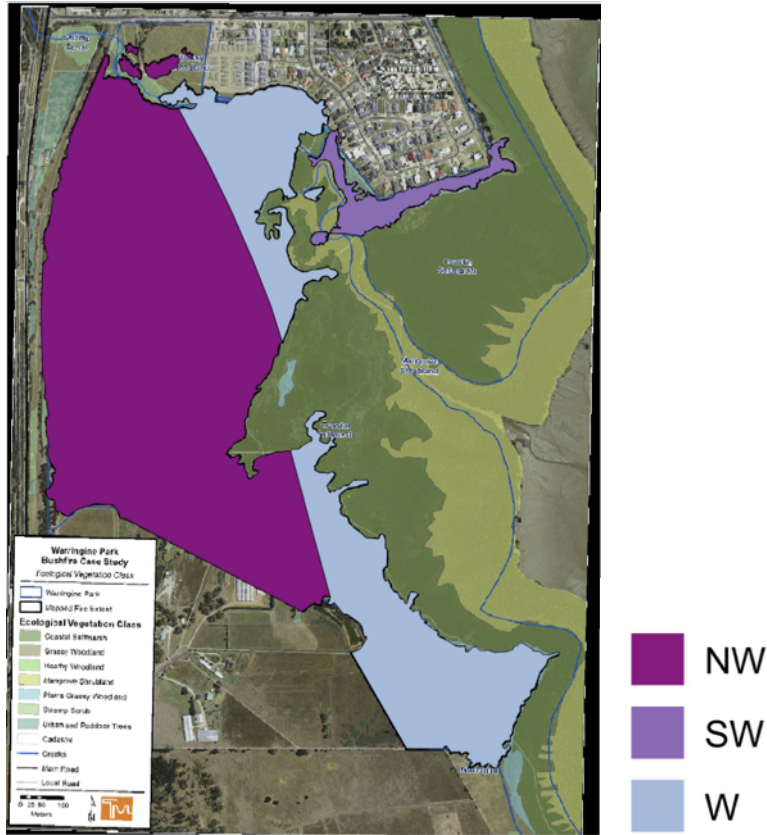
Figure 5: Assumed wind direction for the Warringine Park bushfire case study, for each of the burnt areas in the reserve, adapted from Terramatrix (2015b, Map 5 & 6), overlaying the ecological vegetation map from Terramatrix (2015b, Map 2) to illustrate the proximity of the fire to the residential properties. The western region is assumed to have all burnt under a north westerly wind, the central region under a westerly wind, with a small region in the north east under a south westerly wind.

in the dominant behaviour of the fire. For our analysis, we include only those factors that would be considered in our model, namely the fuel load and wind direction. To apply Eq. (1) it is first necessary to decompose the reserve into the burnt and unburnt regions, and to identify the wind speed and direction under which each region burnt.

Fig. 5 provides the assumed wind direction under which the head of the fire burnt through an area. Weather information was available from the HMAS Cerebus AWS, which is located approximately 3 km south west of the burnt area of the reserve. The HMAS Cerebus AWS is located at a height of 12.69 m. We note that although Terramatrix (2015b) indicated that the fire first burnt through under a northerly wind, we have assumed the wind was north westerly, as this corresponds with the indicated direction of fire spread. As detailed rates of fire progression through the reserve are unknown, a constant wind speed is assumed for each of the three stages of the fire, namely 37 km/h for the north westerly, 57 km/h for the westerly, and 18 km/h for the south westerly wind. The fuel load assumed for each vegetation class is given in Table 1. The fuel load, together with the distribution of vegetation shown in Fig. 4, is used to form the NDF required by Eq. (3).

Ecological Vegetation Class	Fuel load (t/ha)
Swamp scrub	25
Grassy woodland	25
Grassy plains	9.5
Urban and paddock	1.5
Mangrove swamp	0.1
Coastal saltmarsh	0.1

Table 1

Assumed fuel loads, in tonnes/hectare, for each of the ecological vegetation classes. The fuel loads for Swamp Scrub and Grassy Woodland are given by Terramatrix (2015), however details were not provided for the other vegetation classes, and therefore assumed values, adapted from the literature, were used. Grassy plains calculated from Rachmawati et al. (2015, Table2); Urban and Paddock assumed equivalent to eaten out paddocks as per Tolhust (2009); Mangrove swamp and Coastal saltmarsh assumed as a fuel load was omitted in A2.1 Classification of Vegetation Formations in NSW Rural Fire Service (2006).

329   The ember load is calculated by convolving the fine fuel load burnt by the fire with Eq. (3), under the spatially

330   varying wind speed and direction. As previously noted, ember density has been found to decrease exponentially with

331   distance from vegetation (origin). Tolhurst and Howlett (2003) used a one-dimensional decay rate of 0.007 in their

332   analysis. In their case, property damage extended approximately 500m into the housing. In contrast, property damage

333   in the Warringine Park bushfire was constrained to the first row of houses, or approximately 200m from significant

334   vegetation. We therefore adopted a faster decay rate, and selected $\lambda = 0.5$ m/s, and $\kappa = 0.05$ 1/m to model the

335   Warringine Park bushfire. Consideration of other parameter combinations gave qualitatively consistent results (not

336   shown).

337   A detailed view of the calculated ember load in the vicinity of the damaged properties is given in Fig. 6. In

338   addition, Fig. 6 shows the household level ember load together with the level of damage due to the bushfire as reported

339   in Terramatrix (2015b). Only properties in that first row were damaged from the bushfire, potentially due to the

340   screening effect of other houses. The household level ember load is calculated by summing the ember load across the

341   property. Therefore, the reported household level value is a function of both the localised ember load and the size of

342   the property.

343   Of the 50 properties in the first row of the community considered in this analysis, see Fig. 6, 24 of these properties

344   sustained damage. To investigate the relationship between the reported damage (score of $0-4$) and the ember load, the

345   ember load is divided into five classes. Following min-max normalisation, which scales the property ember load to a

346   score between 0 and 1, the properties are divided into five categories. Normalised ember loads less than 0.2 are assigned

347   Class 1, loads between 0.2 and less than 0.4 are assigned Class 2 etc. Table 2 provides a summary of the number of

348   damaged versus undamaged properties in each ember load class. Of the properties in the highest ember load class four

349   houses were damaged, with all four properties reporting damage in level 3 or 4. Table 3 shows the correspondence

350   between houses in the damage class for each of the ember load classes. The Spearman's Rank Coefficient for the

351   reported damage class and total ember load for the property (see Supplement B) is 0.46, which indicates that increasing
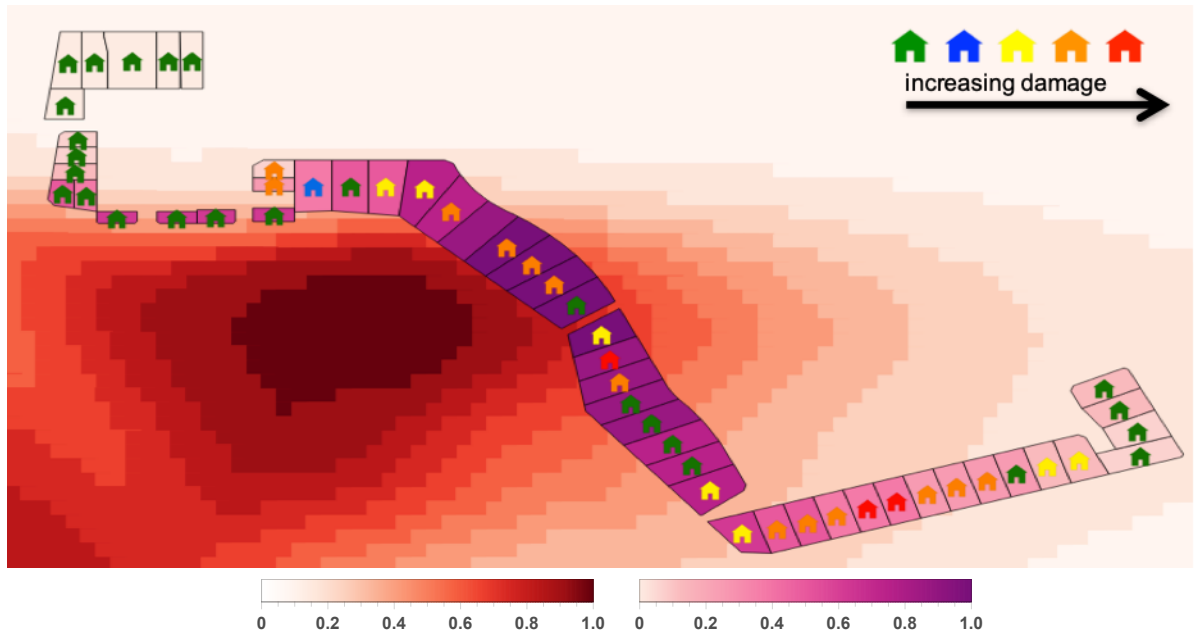
Figure 6: The calculated relative ember load (unit of scaled count per unit area) to the north east of the reserve is shown by the white-red heat map, with darker colours corresponding to a greater ember load (higher ember hazard). The cumulative ember load for houses abutting the reserve is shown by the purple heat map, with higher loads corresponding to darker colours. The house icons indicate the level of damage reported by Terramatrix (2015, Table 12), with green corresponding to a rating of 0 (no observed damage) and red corresponding to a level of 4 (observable damage to dwelling).

Ember load class	Number of houses damaged (%)	Number of houses undamaged (%)
5	4 (57)	3 (43)
4	2 (50)	2 (50)
3	1 (100)	0*
2	5 (83)	1 (17)
1	12 (38)	20 (62)

Table 2
Comparison of damaged and undamaged properties by ember load class for Warringine Park bushfire case study. ∗ One property in ember load class 3 sustained no damage, however this property was vacant (no house) at the time of the bushfire, and has therefore been excluded from this comparison.

352 levels of observed damage correspond to higher ember loads. This relationship is far from perfect, and demonstrates

353 that the calculated ember load should not be considered in isolation. Although parameterisation of the model may

354 produce a higher correlation, over-parameterisation of the model to match the outcomes of a single event should be

355 avoided.

356 Many factors that influence the experienced damage due to embers from a wildfire have been excluded from this

357 analysis, including the resilience of the property to ignition from embers (e.g. construction materials, garden vegetation,

358 household features etc.) as well as any defensive action taken by residents or the Country Fire Authority. Interviews

359 with residents as part of the review were aggregated. It was therefore not possible to use this information to determine

360 whether individual properties were better prepared to withstand ember attack. Resident interviews indicated that at

Ember risk model for households

Damage Class Ember Class	0	1	2	3	4	Total
1	20	1	3	6	2	32
2	1	0	2	3	0	6
3	0*	0	1	0	0	1
4	2	0	1	1	0	4
5	3	0	0	3	1	7
Total	26	1	7	13	3	50

Table 3
Comparison of properties by ember load class and damage class for Hastings Bushfire Case Study. ∗ One property in ember load class 3 sustained no damage, however this property was vacant (no house) at the time of the bushfire, and has therefore been excluded from this comparison.

least 13 of the 23 residents interviewed had performed actions that would improve the resilience of their property to embers. For example, 13 residents reported that they had 'installed seals and/or draft protectors around windows and doors to prevent ember entry', six residents reported installing wire mesh screens (not aluminium) over doors and windows not protected by shutters, and 21 residents reported clearing their gutters of dry leaves (Table 14, Terramatrix 2015b). It is not known which houses were actively defended. Moreover, factors such as the ember intensity, that is the rate at which embers land at a property, has also been neglected, which has significant implications for the defensibility of a property. A further factor neglected from this analysis is the spread of fire between properties. It is noted that many of the damaged properties (level 3 and 4) lie in a roughly east-west line. It is possible that ignited structures would spread the fire from one property to the next, driven by the westerly or south westerly wind. Despite these limitations, this case study has demonstrated that the concept of an ember load can be useful, and supports the use of this model to assist in understanding wildfire risk in communities.

2.2. Long-range embers

Although the majority of ember transport is short-ranged, embers have been observed to create spot fires more than 30km ahead of the fire front (Cruz et al., 2012). Such long-range embers are entrained in the fire plume, and once reaching the top of the plume being carried subject to the background winds. Long-range embers present two distinct, although related, risks to properties. Embers that fall on vulnerable parts of the property, such as evaporative air conditioning units, can lead to a local ignition and subsequent spread to the main structures. A secondary risk from long-range embers is the acceleration and distortion of the fire front due to spotting. While spotting into nearby vegetation is not explicitly modelled as a component of risk, such risk is implicitly included through the combination of long and short-range ember load.

Due to the different mechanisms for long and short-range ember spread, the PDF that describes the resulting ember distribution differs. Thurston et al. (2014) investigated the lateral (transverse) and longitudinal (wind-direction) spread of embers due to interactions between a plume updraft and the background wind speed, for wind speeds between 5 and

15 m/s. Based on their findings, we assume a PDF of the form

$$\rho_{E_{\text{long}}}(x, y) = \frac{1}{2\pi N \sigma_x \frac{\sigma_y x}{\mu_x}} \exp\left[-\frac{1}{2}\left(\left(\frac{x - \mu_x}{\sigma_x}\right)^2 + \left(\frac{y - \mu_y}{\sigma_y x/\mu_x}\right)^2\right)\right], \tag{5}$$

where μ_x is the mean of the distribution in the x direction (wind-direction), the mean in the transverse direction is $\mu_y = 0$ as the ember dispersal is symmetric about the line of the wind direction, and σ_x and σ_y are the standard deviations of the distribution in the x and y directions respectively. The normalisation constant N is defined so that

$$\int_0^\infty dx \int_{-\infty}^\infty \rho_{E_{\text{long}}}(x, y) = 1, \tag{6}$$

with the result that

$$N = \frac{1}{2}\left(\text{erf}\left(\frac{\mu_x}{\sqrt{2}\,\sigma_x}\right) + 1\right). \tag{7}$$

The PDF (5) is a modification of the two-dimensional normal PDF, where the transverse dispersion in the y direction is modified to be a function of x. This modification results in the wedge shape characteristic of Thurston et al.'s (2014) results. The means and standard deviations are all taken to be linear functions of the background wind speed, where the curve has been fitted to the values for the 5 and 15 m/s wind speeds provided by Thurston et al. (2014). That is, with $\mu_x = 0.2u + 1.3$, $\mu_y = 0$, $\sigma_x = 0.08u + 0.41$ and $\sigma_y = -0.0082u + 0.591$, where u is the wind speed. The assumption of a linear relationship between the dispersion parameters and the wind speed is likely an approximation of the true relationship. However, exploration of a quadratic relationship did not yield qualitatively different results. The adjusted normal PDF was selected as it represents the key features of ember dispersal identified in Thurston et al. (2014). It is noted that alternative PDFs, that also share these key features, could have been selected.

Fig. 7 shows the assumed PDF for three chosen wind speeds. One limitation of this approach is that the numerical experiment of Thurston et al. (2014) assumes the plume is independent of the wind speed, however we expect that higher wind speeds will result in more intense plume activity.

As with short-range embers, the ember load for a property due to a forest distribution is obtained by convolving the ember PDF, $\rho_{E_{\text{long}}}$, with the forest NDF, η_F, as per Eq. (1). This is illustrated for a simulated region in Fig. 8, which shows a lower wind speed of 2 m/s that poses a negligible threat to the housing estate, and a considerably higher wind speed of 10 m/s, where embers are expected to impact the housing estate and represents an elevated wildfire risk, particularly in the north west of the estate. These results show that while the risk due to embers follows the generic rule of proximity to forest resulting in higher risk, the true picture is more complicated. Transverse spread of the embers, dependent on the wind speed and direction, together with the accumulation of embers from a depth of forest,
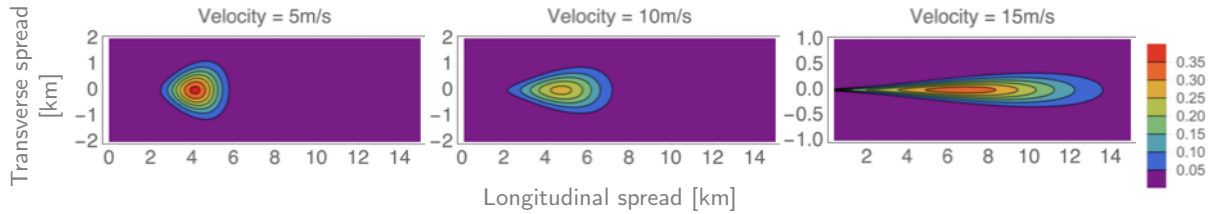
Figure 7: Long-range ember PDF for three selected background wind speeds. The warmer colours correspond to high concentrations of embers while the cooler colours correspond to lower concentrations of embers. The PDF is the proportion of embers per unit area. Embers are released from the origin (0,0) and the x- and y-axes are measured in km.
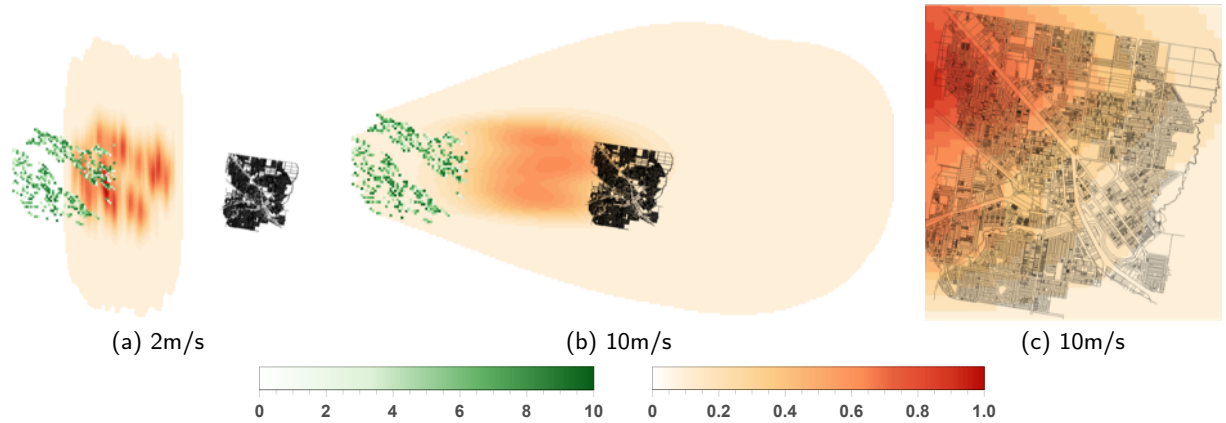

Figure 8: Long-range ember load for a housing estate due to a region of bushland upwind of the estate subject to two different background wind speeds in the positive x direction (westerly wind). The assumed fuel load is indicated by a white-green heat map with higher fuel loads indicated by darker colours. (c) provides a close-up of the risk at the housing estate from the 10m/s background wind scenario shown in (b). The expected load is indicated by a white-red heat map with darker colours corresponding to a higher ember load, and hence risk. The same colour map is used for all three subfigures.

shows that the two-dimensional features of the forest are important to understanding risk. In contrast, risk assessment processes such as the Bushfire Attack Level (NSW Rural Fire Service, 2012) employ a minimum distance rule, where the risk due to local vegetation is a function of the minimum distance between the property and vegetation, without consideration for the spatial extent, or total area, of that vegetation. The distribution of fuel load within the mapped area of forest results in a higher expected ember load to the north west of the estate rather than the south west, which is marginally closer to the forest, as shown in Fig. 8c. In addition to the community level hazard, the information used to form the visualisations in Fig. 8 can be used to identify the level of hazard for an individual property as in Fig. 6, and to map this hazard as a function of the wind speed and direction, in an analogous manner to Fig. 3. Fig. 9 shows just such an example for a property surrounded by forest, but maintaining a large buffer of low fuel load vegetation around the property. Such mappings can be used to highlight the risk posed by embers even at some distance from the forest. Property damage in residential areas has at times taken residents and agencies by surprise, with damage extending beyond the fringes of the community. However, once fire establishes within a community it can rapidly spread between
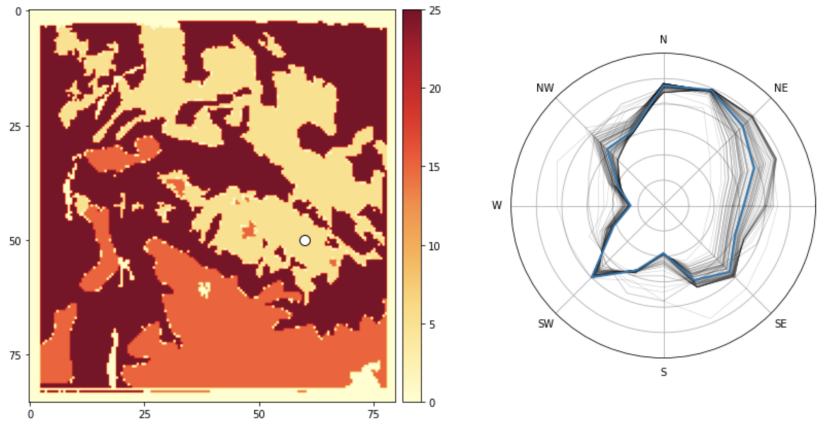
Figure 9: Directional ember load (units of scaled count per unit area) for a selected property, indicated by the white dot in the left-hand image, with a variable background wind speed, and a variable fuel load (t/ha). The circular plot indicates the wind direction corresponding to the scaled risk. The darker colours correspond to a higher fuel load, with lighter colours corresponding to a lower fuel load, the fuel load is indicated by the heat bar, with the darker brown corresponds to a fuel load of 25t/ha, the orange to a fuel load of 15t/ha, and the lighter yellow to fuel loads of 2t/ha. The x and y axes show the relative positions in km within the area of interest, an area of approximately 80km x 80km. The potential ember load is calculated considering long-range processes only. That is, with the ember PDF given by Eq. (5). A Monte Carlo simulation with 100 runs is used to explore sensitivity to the windspeed, u, with each grey line corresponding to a single run. The windspeed is sampled from a Gaussian distribution with a mean of 15 m/s and standard deviation of 5 m/s. The blue line indicates the result with $u = 15$ m/s.

structures. House-to-house spread is driven by direct flame contact and radiation from ignited structures (including wooden fences, sheds, etc.) as well as ember storms from burning structures and garden vegetation. Once multiple properties within a community are ignited, fire defence is challenged as defenders (including fire agencies) are rapidly overwhelmed and unable to respond to all fires simultaneously.

Fig. 9 also provides a sensitivity analysis of the long-range PDF to the windspeed. The Monte Carlo simulation results, which explored windspeeds sampled from a Gaussian distribution with a mean of 15 m/s and standard deviation of 5 m/s, shows that greater variation is evident from wind directions corresponding to high risk than those corresponding to comparatively lower risk. This indicates that homeowners, or councils and agencies, should not consider just a single design event but a range of plausible windspeeds in their decision making.

3. Software Framework

The ember risk model, delivered via a community planning tool such as the PREP app, provides an opportunity to improve community understanding of the role of embers in wildfire risk. In this section we describe the software framework that we developed to support the ember risk modelling. As the ember risk model provides just one element of the risk due to wildfires, it should not be considered in isolation. This section therefore shows how the ember risk module fits into this wider software framework.

We adopt a plug-and-play approach (i.e., the underlying model formula can be replaced) to support continued

Data	Source	Type/Format	Resolution	Update Rate
Address	Open	Point/Shapefile	NA	Static
Elevation	Open	Raster/GTiff	25 m	Static
Vegetation	Open	Polygon/Shapefile	NA	>Yearly
Weather	BOM	Grid	5 km	1-15 minute
Drought Factor	ADFD	Grid/NetCDF	3-6 km	Seasonally
House specification	User	JSON	NA	Semi-static

Table 4
Overview of input data. BOM is the Australian Government Bureau of Meteorology and ADFD is the BOM Australian Digital Forecast Database Grid.

development of understanding of wildfire risk. We present the raw data inputs as well as the data processing tasks. Refer to Wang et al. (2017) for further detail about the software framework.

3.1. Raw Data Inputs

We calculated a series of attributes that are physically based and quantifiable, including distances between property addresses and the adjacent bushland, surrounding tree coverage, and local slope. To obtain these variables, we used the most detailed geospatial datasets available, such as geocoded street addresses, 5km spatial resolution weather data and 25m resolution digital terrain models. These variables together with information provided by the user through our designed mobile app, such as building and roof material, feed into our model to calculate the wildfire risk for each property address. The ember risk module takes in the address of each property and a shapefile of vegetation identified via the fuel load. The input data is summarised in Table 4.

3.2. Data Processing

The data processing includes loading data into a distributed file system, re-projecting geographic coordinate system where required, transforming data format if necessary, partitioning and building indexes at local and global level, as well as query and analytics operations. As an example, Fig. 10 illustrates the data processing sequence for dynamic risk modelling, along with data format and projection.

The ember risk model forms one part of the 'Risk Model', and is calculated according to the algorithm in Appendix A.

4. Applicability of the Ember Risk Model

Ember activity is a concern in all jurisdictions experiencing wildfires, including but not limited to Australia, Canada, Greece, Portugal, Spain and the United States of America. Therefore, although the case study and motivation is focussed on Australia, the ember risk model presented in this paper has wider applications in a global context. Incorporating the ember risk within a more comprehensive framework for wildfire risk analysis and management not only
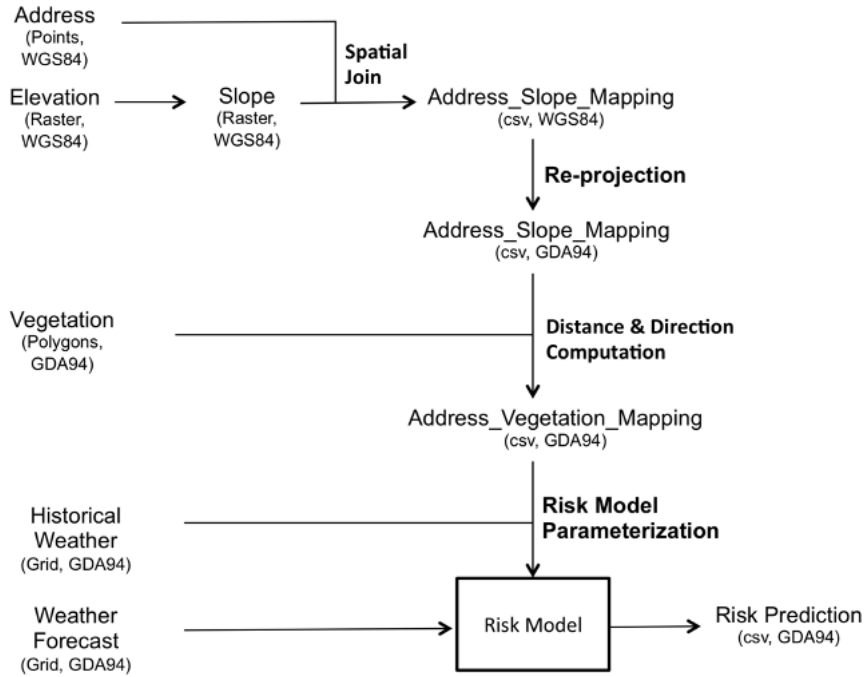
Figure 10: Schematic diagram of data processing steps.

allows for a more accurate evaluation of the potential for losses during wildfires, but provides actionable information to better plan and prepare.

At the community level, maps of ember load can be used by councils and agencies to understand the relative risk posed by different areas of vegetation and thereby inform management practices. This information can also be used in the planning process, to ensure that houses take advantage of design features that will improve the wildfire resilience of the property. This is particularly valuable for new developments, which are most flexible in terms of the orientation and layout of new lots. Roberts et al. (2017) presents a case study of the Ginninderry region, Australia, using this modelling framework, identifying high risk areas within a proposed development that were not required to be built to bushfire standards under the then current building code.

Ember risk information is valuable to individual residents and property owners as it empowers them to make informed decisions about their own wildfire planning and preparation. Understanding the magnitude and direction of their ember risk allows residents to prioritise different mitigation strategies, balanced against the costs of these actions.

Although the ember load model applies in all geographic regions that experience wildfire and significant ember activity, care should be taken when applying the model in a new context. The model is designed to aid planning and improve the representation of embers in wildfire risk evaluations. The model does not predict wildfire behaviour. Local observations of ember activity are required to parameterise the model. Data from multiple events would improve confidence in the parameterisation. Given the inherent uncertainty in parameter selection, a Monte Carlo or similar

approach exploring a range of parameter values is recommended.

5. Summary and Future Work

Analysis of wildfire impacts on properties demonstrates that in Australia embers are the leading cause of house loss, yet management of vegetation and the risk of property damage due to wildfire remains focussed on risks from radiant heat and direct flame contact. Damage resulting from ember activity is common in all regions that experience wildfires, with the degree to which ember risks are managed varying by jurisdiction. This paper presents a new model for the ember hazard component of risk in the form of the ember load. The ember load provides a measure of the relative number of embers that would potentially impact a property during a wildfire, given background wind conditions (speed and direction) and the distribution of vegetation in the region. The presented models have been developed to be scalable, allowing for rapid exploration of different scenarios, to support individualised and community planning. Short- and long-range ember transport is accounted for via two forms of the ember dispersal PDF. The statistical nature of the model avoids the computational complexity and extensive data requirements required for a mechanistic model of ember dispersal. Furthermore, this approach enables the substitution of more physically-based models of both ember production and transport should the necessary computational and data resources be available.

The ember load models use publicly available data sets for weather (wind speed and direction) and vegetation distribution, however a number of simplifying assumptions have been introduced. Future research will focus on relaxing these assumptions to improve the accuracy of the models. In particular, characteristics of the wildfire and their impact on ember generation has not been considered. Presently, the rate and duration of ember activity is neglected, however this will have a considerable impact on the defensibility of a property, and hence the need for structural resilience to prevent damage. More intense wildfires, which can be associated with higher wind speeds or the interaction of wind and terrain, will also generate a greater number of embers from an area of forest than less intense wildfires, and result in larger plumes and consequently embers being released at higher altitudes before being transported via the background wind conditions. The screening effect of trees or other structures on the realised distribution and density of embers has also been neglected. Trees, fences and other structures can serve as a screen, catching embers that would otherwise be transported further from the fire. Such screening provides a protective factor for downwind structures, however results in a large number of embers collecting at the screen, and hence elevating the local risk. This potentially explains the pattern of damage observed during the Warringine Park bushfire, with all damage occurring at the first row of houses.

Here, the models for short and long-range ember dispersal are presented separately, with Eq. (1) showing how the models can be integrated. Roberts et al. (2017) provides an example for the integration of the short and long-range dispersal kernels via a wind-speed dependent function for the proportion of available embers entrained in the plume (long-range dynamics) or transported via short-range dynamics.

Importantly, the ember load should not be considered in isolation. This model is developed to provide just one component of a more comprehensive understanding of wildfire risk to properties. The risks associated with embers can only be realised if the local environment would support a wildfire. Factors such as temperature and humidity are considered in other components of the larger wildfire risk model, and are therefore not explicit within this model. A user must therefore employ a level of judgement when considering the ember load model in isolation from other risk factors – a high windspeed during a rain storm is unlikely to be associated with wildfire activity. It is recommended that, if using this model in isolation to understand the potential ember load, particularly in real-time, that the user first reviews local wildfire ratings. Such systems include the Fire Danger Index in Australia, National Weather Service Red Flag Warnings and Fire Weather Watches in the USA, Canadian Wildland Fire Information System, and the European Forest Fire Information System Fire Weather Index. The ember load can be calculated based on current, or forecast, weather conditions to understand the current or short-term risks. It can also be calculated based on a design event, such as a typical high-risk summer day or a potential catastrophic scenario, to assist with planning. If the weather conditions, real time or modelled, would indicate a resident take action under the local wildfire warning system then considering the ember loads is useful. Outside of these conditions, a wildfire is unlikely to pose a risk to properties, and the concept of a potential ember load makes little sense.

Application of these models to additional case studies is needed, however is limited due to the sparsity of property damage information in the public domain. It was therefore necessary to illustrate the long-range processes via a synthetic dataset. Further case studies would not only provide greater confidence in the application of these models, but coupled with information on the resilience of properties (and any active defence that took place) could provide valuable insights. Such studies could potentially link thresholds in the ember load and realised damage within a community. Additional case studies could also be used to better inform the parameterisation of the models, and verify the selected PDFs. Future research will focus on incorporating additional factors of the wildfire (while maintaining the required computational and data simplicity of the model) and extending the risk measures to include other spatial data sets available.

Our model is simplistic; however, this simplicity is one of design. By focussing on the core factors associated with ember load, the availability of embers and their general pattern of dispersal, data requirements are minimised. Together with a computationally inexpensive solution method, this has resulted in a practically implementable framework that can provide actionable information to residents and communities living in wildfire prone regions.

A. Implementation algorithm for probability density function

Below provides an overview of the steps used by the authors to calculate the ember loads shown in this paper. The exact commands required will depend on the data files used and the programs used to perform the calculations and

visualisations. The authors used QGIS, Microsoft Excel, Mathematica and Python to perform these steps.

Data requirements

To implement this algorithm the following data files are required[2]:

1. Spatial distribution of the fine fuel load. The vegetation in the region is divided into cells of uniform size. The fuel load is assumed to be uniform within each cell.

2. Spatial distribution of properties within the area of interest.

Ember load algorithm

1. Read in the fine fuel load distribution as a matrix **FUELLOADMAT**. The dimensions (Fx, Fy) of **FUELLOAD-MAT** will depend on the size of the region of interest and the resolution for the vegetation that is used.

2. Define the probability density function (PDF) for the ember dispersal, for the wind speed and direction of choice. See below at ⋆ for further details.

3. Decide on the maximum range in the x and y directions at which the PDF will be truncated, that is, the distance from the origin beyond which calculations will not occur and the ember load is assumed to be zero. This distance should be determined with consideration for the range of wind speeds that will be used in future investigations, with consideration for all wind directions.

4. Form the ember dispersal matrix **EMBERDISPMAT** using the same cell size as for the fine fuel load in Step 1. This matrix converts the continuous probability density function into discrete values. That is, calculate the cumulative distribution within each cell and record the value in a matrix, where the row and column indicates the (x,y) distance from the origin. The dimensions (Ex, Ey) of **EMBERDISPMAT** is dependent on the truncation distance determined in Step 6 and the vegetation resolution chosen in Step 1.

5. Extend the size of the **FUELLOADMAT** and **EMBERDISPMAT** by padding with zeros. These two matrices should be extended to the same size. The matrices should have dimensions ($Fx + Ex$, $Fy + Ey$). This ensures that ember dispersal effects from vegetation at the edges of the boundary of interest are captured.

6. Ember dispersal due to the vegetation is the convolution of **FUELLOADMAT** with **EMBERDISPMAT**. Fourier Transforms can be used to speed up the computations. Take the Fourier Transforms of the **FUELLOADMAT** and **EMBERDISPMAT**, which are stored in the matrices **FUELLOADFT** and **EMBERDISPFT**.

7. The **EMBERLOADFT** is given by the element wise multiplication of **FUELLOADFT** and **EMBERDISPFT** (Important: use element wise multiplication, not matrix multiplication).

8. Take the inverse Fourier Transform of **EMBERLOADFT** to obtain the **EMBERLOAD**, the desired result.

---

[2]Data availability varies significantly by region. The authors obtained tree density data from `data.vic.gov.au` for selected council regions in Victoria, Australia, and cadastral property boundaries from `data.gov.au`. Remote sensing methods provide opportunities for new and more up-to-date datasets (see Brandis and Jacobson (2003); Saatchi et al. (2007)). Roberts et al. (2017) related vegetation distribution from Google satellite imagery to typical fuel loads.

566　9. Export **EMBERLOAD**.

567　*Property impact algorithm*

568　1. Import **EMBERLOAD**, converting the cell dimensions to spatial dimensions

569　2. Import vegetation data for visualisation

570　3. Import property data and form property boundaries if required

571　4. Calculate (sum) the total ember load within each property boundary. For larger properties (relative to the resolu-

572　tion chosen in Step 1), other metrics of interest could include the mean and max ember load within the boundary.

573　★ *Wind direction*

574　The dispersal matrix for different wind directions can be produced by rotating the matrix **EMBERDISPMAT** for a given

575　wind speed, or by applying an analytic rotation to the PDF equation, namely $x \rightarrow x \cos\theta - y \sin\theta$, $y \rightarrow x \sin\theta + y \cos\theta$,

576　where θ is the angle of rotation for the wind direction in radians.

577　**B. Supplement**

Damage	Normalised Load	Damage	Normalised Load	Damage	Normalised Load
0	0.000	2	0.094	0	0.225
0	0.005	0	0.095	3	0.243
0	0.006	0	0.106	3	0.253
0	0.010	0	0.107	3	0.313
0	0.017	2	0.110	NA	0.512
0	0.055	0	0.116	2	0.561
0	0.059	3	0.117	0	0.650
0	0.060	2	0.139	3	0.751
3	0.061	3	0.141	0	0.767
0	0.067	4	0.150	2	0.767
0	0.068	1	0.155	3	0.801
0	0.075	3	0.181	0	0.803
0	0.080	0	0.191	3	0.806
3	0.083	3	0.193	0	0.812
0	0.083	4	0.200	0	0.862
0	0.090	2	0.220	4	0.871
0	0.091	2	0.222	3	1.000

Table 5
Calculated normalised ember load for the Warringine Park bushfire case study, see Sec. 2.1 and the reported damage class. Data is arranged in increasing ember load. The property marked 'NA' had no house to sustain damage.

References

Albini, F., 1983. Transport of firebrands by line thermals. Combustion Science and Technology 32.

Alexandridis, A., Vakalis, D., Siettos, C.I., Bafas, G.V., 2008. A cellular automata model for forest fire spread prediction: The case of the wildfire that swept through Spetses Island in 1990. Applied Mathematics and Computation 204, 191–201. doi:`10.1016/j.amc.2008.06.046`.

Allen, T., 2006. Flow over hills with variable roughness. Boundary-Layer Meteorology 121, 475–490. doi:`10.1007/s10546-006-9086-0`.

Anthenien, R.A., Tse, S.D., Carlos Fernandez-Pello, A., 2006. On the trajectories of embers initially elevated or lofted by small scale ground fire plumes in high winds. Fire Safety Journal 41, 349–363. doi:`10.1016/j.firesaf.2006.01.005`.

Baker, E., 2005. Burning characteristics of individual Douglas-fir trees in the wildland urban interface. Master of Science Thesis, Worcester Polytechnic Institute.

Belcher, S.E., Harman, I.N., Finnigan, J.J., 2012. The wind in the willows: Flows in forest canopies in complex terrain. Annual Review of Fluid Mechanics 44, 479–504. doi:`10.1146/annurev-fluid-120710-101036`.

Beringer, J., 2000. Community fire safety at the urban/rural interface: The bushfire risk. Fire Safety Journal 35, 1–23. doi:`10.1016/s0379-7112(00)00014-x`.

Blanchi, R.M., Leonard, J.E., 2005. Investigation of bushfire attack mechanisms resulting in house loss in the ACT bushfire 2003. URL: `http://www.bushfirecrc.com/sites/default/files/managed/resource/act_bushfire_crc_report.pdf`.

Brandis, K., Jacobson, C., 2003. Estimation of vegetative fuel loads using Landsat TM imagery in New South Wales, Australia. International Journal of Wildland Fire 12, 185–194. doi:.`10.1071/WF0303`.

Brenkert-Smith, H., Champ, P.A., Flores, N., 2012. Trying not to get burned: Understanding homeowners' wildfire risk–mitigation behaviors. Environmental Management 50, 1139–1151. doi:`10.1007/s00267-012-9949-8`.

Cal Fire, n.d.a. Fire prevention wildland codes. URL: `http://www.fire.ca.gov/fire_prevention/fire_prevention_wildland_codes`. retrieved 29 June 2018.

Cal Fire, n.d.b. Prepare for wildfire. URL: `http://www.readyforwildfire.org/`. retrieved 20 August 2018.

Chong, D., Tolhurst, K.G., Duff, T.J., 2012. PHOENIX rapidfire 4.0 convection and ember dispersal model. URL: `http://www.bushfirecrc.com/publications/citation/bf-4294`.

Chuvieco, E., Martínez, S., Román, M.V., Hantson, S., Pettinari, M.L., 2013. Integration of ecological and socio-economic factors to assess global vulnerability to wildfire. Global Ecology and Biogeography 23, 245–258. doi:`10.1111/geb.12095`.

Cohen, J., 1995. Structure Ignition Assessment Model (SIAM), in: Weise, D.R., Martin, R.E.c. (Eds.), The Biswell symposium: fire issues and solutions in urban interface and wildland ecosystems; February 15-17, 1994; Walnut Creek, California. Gen. Tech. Rep. PSW-GTR-158. Albany, CA: Pacific Southwest Research Station.

Cohen, J.D., 2012. Residential fire destruction during wildfires: a home ignition problem. URL: `http://www.cmcc.it/wp-content/uploads/2013/04/P_Book_Modelling-Fire-Behaviour-and-Risk.pdf`.

Country Fire Authority, 2011. Landscaping for bushfire. Report no. LFB 11/2011.

Country Fire Authority, 2012. Neighbourhood safer places. URL: `http://www.cfa.vic.gov.au/plan-prepare/neighbourhood-safer-places/`. retrieved 24 July 2017.

Cruz, M.G., Sullivan, A.L., Gould, J.S., Sims, N.C., Bannister, A.J., Hollis, J.J., Hurley, R.J., 2012. Anatomy of a catastrophic wildfire: The Black Saturday Kilmore East fire in Victoria, Australia. Forest Ecology and Management 284, 269–285. doi:`j.foreco.2012.02.035`.

Dold, J., Scott, K., Sanders, J., 2014. The processes driving an ember storm, in: Proceedings of SPEIC14 – Towards Sustainable Combustion, November 19 – 21, Lisboa, Portugal.

El Houssami, M., Mueller, E., Filkov, A., Thomas, J.C., Skowronski, N., Gallagher, M.R., Clark, K., Kremens, R., Simeoni, A., 2016. Experimental procedures characterising firebrand generation in wildland fires. Fire Technology 52, 731–751. doi:10.1007/s10694-015-0492-z.

Ellis, P.F., 2000. The aerodynamic and combustion characteristics of eucalypt bark – a firebrand study. PhD Thesis, Australian National University.

Ellis, P.F., 2003. Spotting and firebrand behaviour in dry eucalypt forest and the implications for fuel management in relation to fire suppression and to "ember" (firebrand) attack on houses, in: 3rd International Wildland Fire Conference, Sydney.

Ganteaume, A., Guijarro, M., Jappiot, M., Hernando, C., Lampin-Maillet, C., Pérez-Gorostiaga, P., Vega, J.A., 2011. Laboratory characterization of firebrands involved in spot fires. Annals of Forest Science 68, 531–541. doi:10.1007/s13595-011-0056-4.

Gibbons, P., van Bommel, L., Gill, A.M., Cary, G.J., Driscoll, D.A., Bradstock, R.A., Knight, E., Moritz, M.A., Stephens, S.L., Lindenmayer, D.B., 2012. Land management practices associated with house loss in wildfires. PLoS ONE 7, e29212–7. doi:10.1371/journal.pone.0029212.

Hall, J., Ellis, P.F., Cary, G.J., Bishop, G., Sullivan, A.L., 2015. Long-distance spotting potential of bark strips of a ribbon gum (Eucalyptus viminalis). International Journal of Wildland Fire 24, 1109–1117. doi:10.1071/WF15031.

Handmer, J., Tibbits, A., 2005. Is staying at home the safest option during bushfires? historical evidence for an Australian approach. Global Environmental Change Part B: Environmental Hazards 6, 81–91. doi:10.1016/j.risks.2005.10.006.

Harris, H., 2011. Analysis and parameterization of the flight of ember generation experiments. URL: https://tigerprints.clemson.edu/all_theses/1251/. Masters Thesis. Graduate School of Clemson University.

Koo, E., Linn, R.R., Pagni, P.J., Edminster, C.B., 2012. Modelling firebrand transport in wildfires using HIGRAD/FIRETEC. International Journal of Wildland Fire 21, 396–417. doi:10.1071/WF09146.

MacAuley, A.S., 2003. An investigation of the impacts of massive short distance spotting on the forward rate of spread of forest fires. Masters of Forest Science Thesis, University of Melbourne.

Manzello, S.L., Cleary, T.G., Shields, J.R., Maranghides, A., Mell, W., Yang, J.C., 2008. Experimental investigation of firebrands: Generation and ignition of fuel beds. Fire Safety Journal 43, 226–233. doi:10.1016/j.firesaf.2006.06.010.

Manzello, S.L., Cleary, T.G., Shields, J.R., Yang, J.C., 2006. On the ignition of fuel beds by firebrands. Fire and Materials 30, 77–87. doi:10.1002/fam.901.

Manzello, S.L., Foote, E.I.D., 2012. Characterizing firebrand exposure from wildland–urban interface (WUI) fires: Results from the 2007 Angora Fire. Fire Technology 50, 105–124. doi:10.1007/s10694-012-0295-4.

Manzello, S.L., Maranghides, A., Mell, W.E., 2007. Firebrand generation from burning vegetation. International Journal of Wildland Fire 16, 458–462. doi:10.1071/WF06079.

Manzello, S.L., Maranghides, A., Shields, J.R., Mell, W.E., Hayashi, Y., Nii, D., 2009. Mass and size distribution of firebrands generated from burning Korean pine (Pinus koraiensis) trees. Fire and Materials 33, 21–31. doi:10.1002/fam.977.

Manzello, S.L., Suzuki, S., 2013. Experimentally simulating wind driven firebrand showers in wildland-urban interface (WUI) fires: Overview of the NIST firebrand generator (NIST Dragon) technology. Procedia Engineering 62, 91 – 102. doi:10.1016/j.proeng.2013.08.047. 9th Asia-Oceania Symposium on Fire Science and Technology.

Maranghides, A., Mell, W., 2010. A Case Study of a Community Affected by the Witch and Guejito Wildland Fires. Fire Technology 47, 379–420. doi:10.1007/s10694-010-0164-y.

McCaffrey, S., 2015. Community wildfire preparedness: a global state-of-the-knowledge summary of social science research. Current Forestry Reports 1, 81–90. doi:10.1007/s40725-015-0015-7.

NSW Rural Fire Service, 2006. Planning for bush fire protection. ISBN: 0 9751033 2 6.

NSW Rural Fire Service, 2012. BAL risk assessment application kit new dwellings and alterations and additions to existing dwellings. ISBN: 0

654   9751033 2 6.

655   Papakosta, P., Xanthopoulos, G., Straub, D., 2017. Probabilistic prediction of wildfire economic losses to housing in Cyprus using Bayesian network
656   analysis. International Journal of Wildland Fire 26, 10–14. doi:10.1071/WF15113.

657   Perryman, H.A., Dugaw, C.J., Varner, J.M., Johnson, D.L., 2013. A cellular automata model to link surface fires to firebrand lift-off and dispersal.
658   International Journal of Wildland Fire 22, 428–439. doi:10.1071/WF11045.

659   QGIS, 2015. Quantum GIS. URL: http://qgis.org/en/site/. version 2.8.3-Wien.

660   Quarles, S., Smith, E., 2011. The Combustibility of Landscape Mulches. Technical Report SP-11-04. URL: https://www.unce.unr.edu/
661   publications/files/nr/2011/sp1104.pdf.

662   Quill, R., Sharples, J.J., Sidhu, L.A., 2019. A statistical approach to understanding canopy winds over complex terrain. Environmental Modeling
663   & Assessment doi:10.1007/s10666-019-09674-w.

664   Rachmawati, R., Ozlen, M., Reinke, K.J., Hearne, J.W., 2015. A model for solving the prescribed burn planning problem. SpringerPlus 4, 384–21.
665   doi:10.1186/s40064-015-1418-4.

666   Roberts, M.E., Sharples, J., Rawlinson, A., 2017. Incorporating ember attack in bushfire risk assessment: a case study of the Ginninderry region,
667   in: Syme, G., Hatton MacDonald, D., Fulton, B., Piantadosi, J. (Eds.), Proceedings of the 22nd International Conference on Modelling and
668   Simulation, Hobart, Tasmania, Australia, pp. 1–8. URL: http://www.mssanz.org.au/modsim2017/H10/roberts.pdf.

669   Rothermel, R., 1983. How to predict the spread and intensity of forest and range fires. Technical Report General Technical Report INT-143. USDA
670   Forest Service, Intermountain Forest and Range Experiment Station.

671   Saatchi, S., Halligan, K., Despain, D.G., Crabtree, R.L., 2007. Estimation of forest fuel load from radar remote sensing. IEEE Transactions on
672   Geoscience and Remote Sensing 45, 1726–1740.

673   Standards Australia, 2009. AS 3959, Australian Standard for construction of buildings in bushfire prone areas.

674   Suzuki, S., Manzello, S.L., Lage, M., Laing, G., 2012. Firebrand generation data obtained from a full-scale structure burn. International Journal of
675   Wildland Fire 21, 961–968. doi:10.1071/WF11133.

676   Syphard, A.D., Keeley, J.E., Massada, A.B., Brennan, T.J., Radeloff, V.C., 2012. Housing arrangement and location determine the likelihood of
677   housing loss due to wildfire. PLoS ONE 7, e33954–13. doi:10.1371/journal.pone.0033954.

678   Tarifa, C.S., del Notario, P.P., Moreno, F.G., 1965. On the flight paths and lifetimes of burning particles of wood, in: Proceedings of the Combustion
679   Institute, p. 1021–1037.

680   Terramatrix, 2015. Hastings bushfire case study Warringine Park (Coastal Section). Summary of Findings. Report to Mornington
681   Peninsula Shire Council and Country Fire Authority. Technical Report. URL: http://www.mornpen.vic.gov.au/files/
682   67e834d8-eb54-4fb4-a8d8-a53200e9e060/Hastings_Bushfire_Case_Study_Executive_Summary_-_Warringine_Park_--
683   Final.pdf.

684   Terramatrix, 2015b. Hastings bushfire case study Warringine Park (Coastal Section). (MPSC- 2015-2 Hastings PIA). Report to Morn-
685   ington Peninsula Shire Council and Country Fire Authority. Technical Report. URL: http://www.mornpen.vic.gov.au/files/
686   cf905475-dbb3-4aea-ac04-a53200e9c482/Hastings_Bushfire_Case_Study_-_Warringine_Park_-_Final_Version.pdf.

687   Thurston, W., Kepert, J.D., Tory, K.J., Fawcett, R.J.B., 2017. The contribution of turbulent plume dynamics to long-range spotting. International
688   Journal of Wildland Fire 26, 317–330.

689   Thurston, W., Tory, K.J., Kepert, J.D., Fawcett, R.J.B., 2014. The effects of fire-plume dynamics on the lateral and longitudinal spread of long-
690   range spotting, in: Proceedings of the Research Forum at the Bushfire and Natural Hazards CRC AFAC conference, Wellington. doi:10.1071/
691   WF16142.

Tolhurst, K.G., Howlett, K.A., 2003. House ignition likelihood index - an risk assessment method for land managers in the wildland-urban interface, in: 3rd International Conference on Wildland Fire, Sydney, Australia. URL: http://www.fire.uni-freiburg.de/summit-2003/3-IWFC/Papers/3-IWFC-075-Tolhurst.pdf.

Tolhust, K., 2009. Report on the physical nature of the Victorian fires occurring on 7th February 2009.

Wang, H.H., 2011. Analysis of downwind distribution of firebrands sourced from a wildland fire. Fire Technology 47, 321 –340. doi:10.1007/s10694-009-0134-4.

Wang, Z., Roberts, M.E., Rusu, L., 2016. Dynamic and personalised recommendations for proactive bushfire risk management, in: Australian New Zealand Disaster and Emergency Management Conference, pp. 197–212.

Wang, Z., Vo, H., Salehi, M., Rusu, L., Reeves, C., Phan, A., 2017. A large-scale spatio-temporal data analytics system for wildfire risk management, in: Proceedings of the Fourth International ACM Workshop on Managing and Mining Enriched Geo-Spatial Data, pp. 1 – 6.

Westhaver, A., 2017. Why some houses survived: Learning from the Fort McMurray wildland/urban interface fire disaster. URL: https://www.iclr.org/wp-content/uploads/PDFS/why-some-homes-survived-learning-from-the-fort-mcmurray-wildland-urban-interface-fi pdf. accessed 10 December 2019.

Wilson, A.A.G., 1988. A simple device for calculating the probability of a house surviving a bushfire. Australian Forestry 51, 119–123. doi:10.1080/00049158.1988.10674524.

Wilson, A.A.G., Ferguson, I.S., 1984. Fight or flee?—a case study of the Mount Macedon bushfire. Australian Forestry 47, 230–236. doi:10.1080/00049158.1984.10676007.

Woycheese, J.P., Pagni, P.J., Liepmann, D., 1999. Brand propogation from large-scale fires. Journal of Fire Protection Engineering 10, 13 – 44.

Zhou, K., Suzuki, S., Manzello, S.L., 2015. Experimental study of firebrand transport. Fire Technology 51, 785–799. doi:10.1007/s10694-014-0411-8.

Highlights

- Developed new household level model for risk posed by embers
- Scalable model with minimal data requirements
- Application of the model demonstrated for the 2015 Warringine Park bushfire, Victoria, Australia